Permeability and chemical analysis of aromatic polyamide based membranes exposed to sodium hypochlorite

Axel Ettori, Emmanuelle Gaudichet-Maurin, Jean-Christophe Schrotter, Pierre Aimar, Christel Causserand

Permeability and chemical analysis of aromatic polyamide based membranes exposed to sodium hypochlorite

Axel Ettori[a,b,c,*], Emmanuelle Gaudichet-Maurin[c], Jean-Christophe Schrotter[c], Pierre Aimar[a,b], Christel Causserand[a,b]

[a] Université de Toulouse, INPT, UPS, Laboratoire de Génie Chimique, 118 route de Narbonne, F-31062 Toulouse cedex 09, France
[b] CNRS, Laboratoire de Génie Chimique, F-31062 Toulouse, France
[c] Veolia Environnement Research and Innovation, Water Research Center, Chemin de la digue, BP76, 78603 Maisons-Laffitte cedex, France

A B S T R A C T

In this study, a cross-linked aromatic polyamide based reverse osmosis membrane was exposed to variable sodium hypochlorite ageing conditions (free chlorine concentration, solution pH) and the resulting evolutions of membrane surface chemical and structural properties were monitored. Elemental and surface chemical analysis performed using X-ray photoelectron spectroscopy (XPS) and Fourier transform infrared spectroscopy (FTIR), showed that chlorine is essentially incorporated on the polyamide layer of a commercially available composite RO membrane, when soaked in chlorine baths, presumably through a two step electrophilic substitution reaction governed by the concentration of hypochlorous acid (HOCl), at pH values above 5. Deconvolution of the FTIR vibrational amide I band experimentally confirmed previous assumptions stated in the literature regarding the weakening of polyamide intermolecular hydrogen bond interactions with the incorporation of chlorine. An increase in the fraction of non associated C═O groups (1680 cm^{-1}) and a decrease of hydrogen bonded C═O groups (1660 cm^{-1}) were observed with an increase in the concentration of the free chlorine active specie. The relative evolution of pure water permeability was assessed during lab-scale filtration of MilliQ water of a membrane before and after exposure to chlorine. Filtration results indicate polyamide conformational order changes, associated with the weakening of polyamide intermolecular H bonds, as observed with the increase in the packing propensity of the membrane, dominant for HOCl doses above 400 ppm h. In addition, water–sodium chloride selectivity capabilities permanently decreased above this HOCl concentration threshold, further suggesting polyamide chain mobility. However, under controlled exposure conditions, i.e., HOCl concentration, operating conditions (applied pressure or permeation flux) can be improved while maintaining similar RO membrane separation performance.

1. Introduction

Aromatic polyamide thin films, synthesized by interfacial polymerization, are currently the base of commercially available composite reverse osmosis membranes (RO). This polymer acts as the membrane active layer in applications including seawater desalination, water reclamation and reuse, and several other purification processes [1–3]. During the course of their use, RO membrane selectivity and production capabilities progressively abate, significantly affecting their operating lifetime onsite. Fouling, consisting namely of contributions from colloidal cake fouling, biofouling and inorganic deposition (scaling) or combination of these, is considered to be the main cause for the decrease of membrane operation efficiency, e.g., with a reduction of permeation flux [4–7]. Chemical cleaning is performed periodically to mitigate membrane performance loss. Generally, alkaline and acidic based cleaning agents (generic or formulated) are used on-site [8]. Sodium hypochlorite, a disinfecting agent commonly used during chemical backwashes of ultrafiltration or microfiltration membranes [9,10], has been assessed as a means to control RO membrane biofouling [11]. However, the ubiquitous reactivity of aromatic polyamide with chlorine is evident from ample published literature on this topic [12–15]. Membrane manufacturers unanimously recommend minimizing exposure, such that free chlorine concentration be below 0.1 mg L^{-1}, as can be found on RO membrane technical data sheets [16,17].

Chlorination of aromatic polyamide has been studied on model compounds, namely benzanilide, acetalinide and derivatives, mim-

* Corresponding author at: Veolia Environnement Research and Innovation, Water Research Center, Chemin de la digue, BP76, 78603 Maisons-Laffitte cedex, France. Tel.: +33 5 61 55 76 19; fax: +33 5 61 55 61 39.
E-mail address: axel.ettori@veolia.com (A. Ettori).

icking main polyamide chemical functions [18,19]. Admittedly, the reaction mechanism involves a two-step electrophilic substitution, consisting of an N-chlorination (a reaction extensively studied on amines and amides [20,21]), reversible and instantaneous, followed by a ring-chlorination, an irreversible reaction, occurring on the meta-substituted phenylenediamine aromatic cycle through Orton rearrangement and yielding no chain cleavage [22]. This reaction is favored at acidic pH, where the hypochlorous acid and aqueous chlorine, free chlorine specie are dominant [19,23]. A direct ring chlorination pathway has also been suggested as cited in the article of Glater et al. (1994) [18] although the reaction involves aqueous chlorine and requires the presence of a catalyst such as a Lewis acid, known to govern eletrophilic aromatic substitution reactions [24].

Polyamide RO membrane solute rejection and water transfer were monitored in pilot test studies to assess the impact of exposure to chlorine and monochloramine, when added into the influent groundwater or surface water upstream of the RO modules [11,25,26]. These studies particularly reported solute rejection loss with increasing free chlorine contact time during long term filtration and ageing studies.

Spectroscopic analysis of commercially available composite RO membranes, namely Fourier transform infrared red (FTIR) and X-ray photoelectron spectroscopy (XPS), were used to study aromatic polyamide chemical modifications with exposure to chlorine [15,27]. Results of these studies support the chlorination mechanism of aromatic polyamide, presented previously, and IR polyamide band modifications were correlated to the evolution of membrane transfer properties with varying chlorine ageing conditions (free chlorine concentration and solution pH). Membrane performance alterations, as observed in pilot studies and in a recent work on the NF/RO rejection of trace pharmaceutically active compounds, such as carbamazepine and ibuprofen [28], can thus be related to intrinsic aromatic polyamide property modifications during chlorine ageing. In a study on the evolution of aromatic polyamide specific vibrational IR bands, Kwon et al. hypothesized that the incorporation of chlorine results in the weakening of aromatic polyamide intermolecular hydrogen bond (H bond) interactions, presumably with the substitution of N–H···O═C by N–Cl O═C [29,30]. The disruption of these physical interactions, classified as weak interactions [31], was further believed to promote local chain mobility, accounting for the water flux variations with applied pressure and/or permeation of sodium chloride, as reported in lab-scale filtration studies [29].

H bond interactions have been shown to contribute to aliphatic polyamide structural order and phase transition properties, as reported in studies on semicrystalline and fully amorphous nylons [31–35]. The effect of stress, heat and solvent-induced changes on conformational order and enhancement of chain motion and free volume was demonstrated with various spectroscopy techniques and X-ray diffraction crystallography and was shown to be related to the disruption of intermolecular H bonds. In the study of the underlying risk of a loss of polyamide-based RO membrane selectivity capabilities, there is a strong need to demonstrate that exposure of these membranes to free chlorine results in the weakening of H bond interactions within the aromatic polyamide structure.

The purpose of the present study was to assess structural modifications of rigid aromatic polyamide RO membranes exposed to varying chlorine ageing concentrations. Membrane hydraulic resistance, a membrane property influenced (amongst others) by the physicochemical interactions with environing species, and by chain conformation of the polymer used as the filtration active layer, was monitored during ultrapure water filtration tests performed under high-pressure. Correlation between membrane transfer property modifications and the increase of the fraction of non-associated carbonyl groups, an H bond acceptor, obtained by curve fitting of IR spectra is also discussed. Sodium chloride rejection was monitored on initially pristine then aged membranes to provide additional insights of polyamide based RO membrane transfer property modifications with exposure to chlorine.

Table 1
Free chlorine (HOCl and ClO^-) content as a function of pH.

	pH 5.0	pH 6.9	pH 8.0	pH 12
% HOCl	100	78	22	0
% ClO^-	0	22	78	100

2. Experimental

2.1. Material

Experiments were performed with high-pressure composite reverse osmosis membranes SW30HRLE-400 (Dow FILMTEC™). According to the manufacture, these membranes have a thin active layer made of fully aromatic crosslinked polyamide synthesized on a polysulfone porous layer supported by a polyester backing layer.

2.2. Sample preparation

All membrane samples were extracted from an 8″ spiral wound module, stored at 4 °C. These samples were then thoroughly rinsed with MilliQ water and soaked in MilliQ water baths for 24 h to remove preservation agents prior to characterization and/or ageing (total organic carbon of baths after immersion was below 0.5 mg C L^{-1}). Water baths were periodically renewed and a final bath was stored overnight at 4 °C. Samples used for polymer chemical and elemental composition (determined by attenuated total reflection Fourier transform infrared spectroscopy ATR-FTIR, and X-ray photoelectron spectroscopy XPS) were in addition dried in a vacuum before analysis.

2.3. Chlorine solution and accelerated ageing method

The chlorine solution was prepared by diluting a 111 g L^{-1} NaOCl commercial bleach solution in MilliQ water (resistivity of 18.2 MΩ cm) to the desired concentrations, ranging from 0.54 to 54 mM NaOCl (i.e., 40–4000 mg L^{-1}). Free chlorine concentration (mainly hypochlorite ion at natural sodium hypochlorite pH, ca. pH of 11.5–12.0) of a diluted aliquot was spectrophotometrically determined (λ_{max} = 292 nm, ε_{max} = 348 M^{-1} cm^{-1}).

The pH of the solution was adjusted by addition of hydrochloric acid 37% (v/v) (Acros Organics) to the desired pH of 6.9 or 8.0 corresponding to pH conditions found in seawater desalination plants. The process was monitored with a pH meter (WTW, Sensitix 41). Additionally, ageing was performed at pH 5.0 and 12, where hypochlorous acid and hypochlorite ion are, respectively, dominant, to provide complementary insights on the chlorine reaction mechanism of polyamide based RO membranes. Contents of free chlorine species at each pH are given in Table 1 (obtained from the free chlorine fraction vs. pH diagram and spectrophotometrically verified for HOCl [λ_{max} = 230 nm, ε_{max} = 111 M^{-1} cm^{-1}] and ClO^- [λ_{max} = 292 nm, ε_{max} = 348 M^{-1} cm^{-1}]).

Ageing experiments were performed at 20 ± 3 °C by soaking, in static conditions, membrane samples in 1 L borosilicate glass beakers covered with Parafilm™ and stored in a dark area to reduce natural chlorine reaction with light or air. Contact time, unless specified otherwise, was set to 1 h. The total exposure of membrane to chlorine was expressed as ppm h.

On average, less than 5% variation of the free chlorine concentration was noticed (by comparison of the values measured before and after immersion of the membrane samples).

Aged samples were thoroughly rinsed with MilliQ water to remove excess chlorine at the surface of the membrane and stored overnight in MilliQ water at 4 °C prior to analysis.

2.4. Filtration setup and test solution

A cross-flow filtration cell (SEPA II, GE Infrastructure Water and Process Technologies), designed for operation up to 69 bar, was used for the high-pressure filtration characterization experiments. Membrane samples, placed in between the feed spacer and permeat collector (provided with the filtration cell), offered an effective surface area of 140 cm^2. The feed solution was contained in a 10 L stainless steel cylindrical tank, equipped with a double envelope connected to a refrigerated recirculating chiller (Lauda). The temperature of the feed solution was monitored with a thermometer and held at a constant temperature of 25 ± 3 °C. The feed solution was pumped from the tank, pressurized through the filtration cell and circulated back to the feed tank by a hydracell pump (Wanner Engineering).

During salt filtration experiments, permeate and retentate were continuously recycled back to the feed tank, in which the bulk feed salt concentration, monitored using a conductivity meter (WTW, LF 318), and pH (WTW, Sensitix 41) were kept constant. The applied pressure was controlled by a back-pressure regulator (Tescom) and monitored with two pressure gauges (Keller, PA-21S). Through adjustment of a by-pass valve, the flow rate across the filtration cell was controlled (130 L h^{-1} corresponding to a cross-flow velocity of 0.3 m s^{-1}) and was monitored by a gear flowmeter using pulse output (Macnaught, M 2RRP-1C).

Sodium chloride (NaCl) supplied by Acros Organics (purity of 99.5%) was stored and used as received. NaCl solutions were used to determine rejection rates of membrane samples.

2.5. Membrane characterization

2.5.1. Membrane permeability and salt rejection

The filtration protocol used to determine the membrane pure water permeability was applied similarly to membrane samples before and after contact with the chlorine ageing baths.

In brief, MilliQ water was filtered through the membrane at a natural pH (pH ~ 6) and at applied pressures between 55 and 60 bar to allow for membrane compaction. The temperature was maintained at 25 ± 3 °C, the dynamic viscosity of water at this temperature being equal to 0.891×10^{-3} Pa s. Membrane hydraulic resistance was determined after stable flux was achieved (value remained constant for 30 min), by measuring the pure water flux over a range of applied pressures (5, 10, 25, 35 and 45 bar). The relationship governing the experimental pure water flux is:

$$Lp_0 = \frac{J_0}{\Delta P} = \frac{1}{\mu R_m} \quad (1)$$

In Eq. (1), Lp_0 is the membrane pure water permeability (L h^{-1} m^{-2} bar^{-1}), J_0 the pure water flux (L h^{-1} m^{-2}), ΔP is the applied pressure (bar), μ the dynamic viscosity of water (Pa s) and R_m the membrane hydraulic resistance (m^{-1}).

Once the pure water permeability of the pristine membrane was determined, a NaCl aqueous solution was added in the feed tank, to achieve a NaCl concentration of 0.55 M, and filtered through the membrane at a constant permeation flux of 31 L h^{-1} m^{-2} (based on manufacturer membrane test conditions) at 25 °C by adjusting the applied pressure and with a cross-flow velocity of 0.3 m s^{-1}, corresponding to tangential velocity conditions found on-site [36]. Water permeability (A) during salt filtration and observed salt rejection (R_{obs}) were determined by using Eqs. (2)–(4).

$$A = \frac{J}{(\Delta P - \Delta \pi_b)} \quad (2)$$

$$\Delta \pi_b = iRT(C_b - C_p) \quad (3)$$

$$R_{obs} = 1 - \frac{C_p}{C_b} \quad (4)$$

where $\Delta \pi_b$ is the bulk trans-membrane osmotic pressure (determined using the Van't Hoff equation, Eq. (3)) ($\Delta P - \Delta \pi_b$) is the net driving pressure for permeation (bar), J the permeation flux measured volumetrically in a 20 mL flask and C_b and C_p, respectively the bulk and permeate salt concentrations (expressed in M) determined with a conductivity meter in the feed and permeate solutions. Water permeability and salt rejection were not corrected for the concentration polarization effects. The relative evolution of these membrane bulk transfer properties after exposure to chlorine was the main focus of this paper.

After stable conditions were obtained, these transfer properties were determined. The membrane sample and the filtration cell were then rinsed with MilliQ water until the conductivity in the recirculated feed and in the permeat streams was below 5 μS cm^{-1}. The membrane sample was removed from the filtration cell and stored overnight in MilliQ water at 4 °C. The following day, the same membrane was immersed in the ageing bath, prepared at the desired concentration and pH, for 1 h, was then thoroughly rinsed with MilliQ water to remove excess chlorine at the surface of the membrane and stored overnight in MilliQ water at 4 °C. On the third day the aged membrane was placed in the filtration cell and underwent the similar filtration procedure.

This cycle was carried out once per ageing condition and a new membrane sample was used each time. No repetition of this cycle was performed.

2.5.2. ATR-FTIR

2.5.2.1. Experimental spectra acquisition. Attenuated total reflection-Fourier transform infrared spectra were obtained on a Nexus (ThermoNicolet) spectrometer equipped with an ATR element (45° multi-reflection ZnSe HART 2.38 cm^2 flat plate crystal) and a nitrogen-cooled mercury–cadmium–telluride (MCT) detector for polymer thin-film analysis. The membrane samples were pressed against the ATR crystal plate (with the polyamide skin layer facing the crystal). A minimum of 60 scans acquired between 4000 and 650 cm^{-1} at a resolution of 2 cm^{-1} were signal-averaged. The cell containing the membrane samples was covered and continuously purged with dry air to reduce the interference of atmospheric moisture with the spectra. Spectra were plotted on an absolute absorbance scale. No amplification of the IR bands was performed. Thus, IR band absorbance intensity modifications and frequency shifts could be directly visualized. To minimize possible heterogeneous chlorination on the polyamide surface, IR spectra were taken at different membrane sample locations and for three separate ageing campaigns.

2.5.2.2. Curve fitting. Curve fitting of polyamide specific IR bands was performed with Grams AI software. A flat baseline was applied in the area of IR frequency of interest. Spectra of pristine or chlorine-aged membranes were used without any further modification. Adjustment of curve fitting parameters (namely, modeling of band shape and the number of bands) was performed to obtain a good fitting with the experimental spectra and results chemically and physically relevant. Explanation on the procedure is detailed more in length in Section 4 along with the assignment and description of the IR bands and deconvolutions of interest.

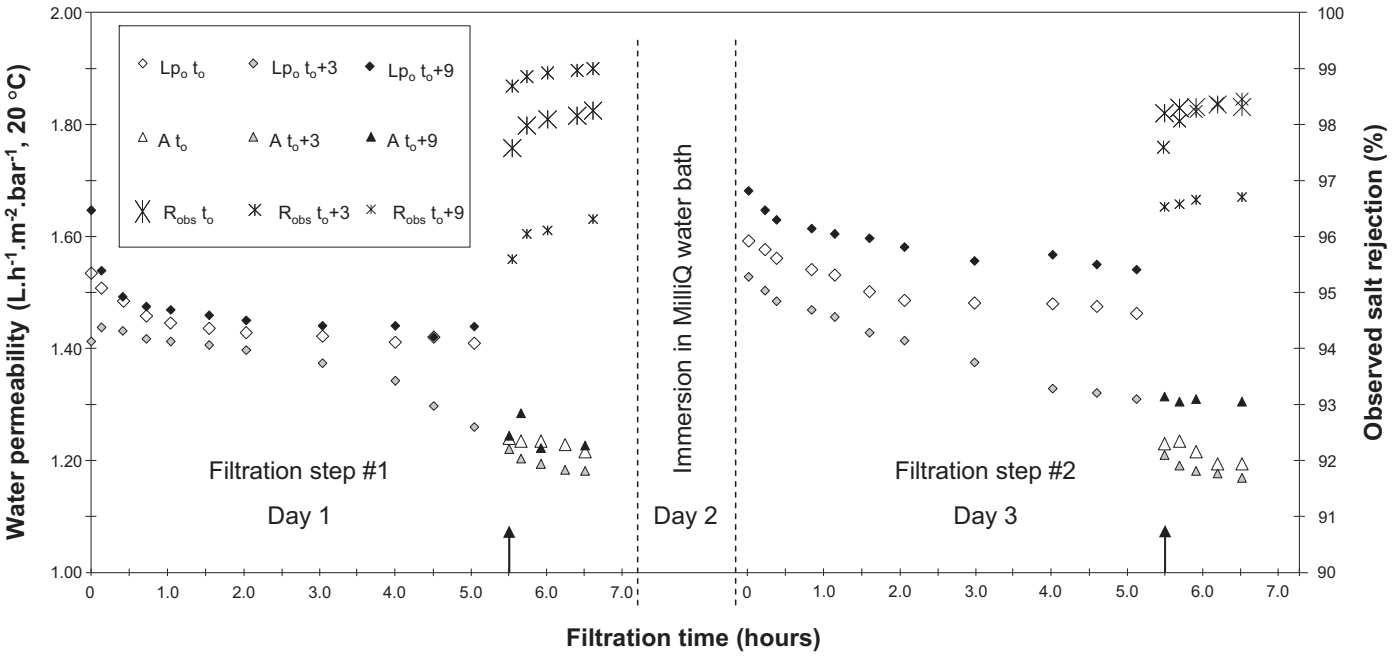

Fig. 1. Pure water permeability (Lp_0), water permeability (A) and NaCl rejection (R_{obs}) during NaCl filtration (0.55 M NaCl, J = 31 L h^{-1} m^{-2}) of pristine RO membranes. Transfer properties remained unchanged throughout the 2 characterization filtration steps and the time span of the experimental campaign, at times t_0, t_0 + 3 months and t_0 + 9 months. ↑Indicates start of salt filtration.

2.5.3. XPS

XPS spectroscopy was performed with an Escalab 250 (Thermo Electron) XPS spectrometer using a monochromatic aluminum $K\alpha$ radiation as an X-ray excitation source (1486.6 eV). A spot of the membrane sample of 400 μm in diameter was scanned using this source. Elemental composition was determined through approximately the top 10 nm in depth of the surface of the samples. Membrane samples were mounted on a sample holder with graphite adhesive tape and kept overnight at high vacuum in the preparation chamber before they were transferred to the analysis chamber of the spectrometer. Avantage software was used for acquisition and data analysis.

Survey XPS spectra were obtained by scanning over a 0–1200 eV electron binding range with an energy step size of 1 eV. High resolution XPS core-level spectra were obtained by averaging 15 scans for C 1s, O 1s, N 1s, S 2p and Cl 2p with an energy step size of 0.2 eV. Membrane samples were irradiated separately and for a maximum time of 15 min. All high resolution scans were normalized against the binding energy of the aromatic C=C bond (C 1s corrected to 284.6 eV). Atomic concentration percentages of C, O, N, S and Cl of the membranes before and after contact with chlorine ageing baths were determined using a semi-quantitative method. The surface atomic concentrations were determined from photoelectron peak areas using the atomic sensitivity factors reported by Scofield. The background signal was subtracted using the Shirley method.

Sample charging was minimized by an electron flood gun operated at 2 eV. Deconvolution of the peaks obtained by XPS was not performed.

3. Setup of filtration and ageing protocols

Accelerated ageing protocols are commonly used to enhance polymer property modifications, e.g., for polymer photo-induced oxidation [37,38]. In most studies published on the chlorine ageing of polyamide RO membranes, this was also the case. High chlorine concentrations were used (at least 10–100 times higher than those usually found in water treatment plants) to perform accelerated ageing experiments. It is difficult to argue whether working in such conditions is relevant to simulate possible chlorine ageing of membranes on-site [28,39]. Several studies found that the chlorination of amine [20] or amide [21] follows a pseudo-first order law relative to the chlorinating agent. This was also found for chlorination studies with B9 aromatic polyamide membranes [40]. Chlorine concentrations used in these studies ranged from 120 to as high as 1000 mg L^{-1} NaOCl at near neutral pH values. We thus assumed that these rate laws were applicable to conditions used in our study and that chlorine ageing conditions performed at different concentrations but at the same doses (expressed as ppm h) should lead to similar modifications of membrane physical–chemical properties. One of the advantages of working over such a wide chlorine dose range, other than exacerbating the response of membrane ageing at high doses, is to be able to identify one or several chlorine ageing mechanisms and to evaluate the sensitivity of experimental methods and analytical tools used for the characterization.

3.1. Filtration control tests

Transfer properties of initially pristine membranes (having not been used or exposed to cleaning agents prior to characterization) were determined during high-pressure filtration experiments (Fig. 1). A stable pure water permeability (on average, $Lp_0 = 1.4 \pm 0.1$ L h^{-1} m^{-2} bar^{-1} or $R_m = 2.5 \times 10^{14}$ m^{-1}, 20 °C) was achieved after 5 h of compaction at applied pressures of 55–60 bar. Additional compaction performed up to 10 h (results not shown) lead to a slightly lower value (5% difference). 5 h compaction time was considered sufficient to achieve stabilization of pure water flux in preparation for salt filtration. Water permeability (A) and observed salt rejection (R_{obs}) were, respectively, of 1.2 ± 0.1 L h^{-1} m^{-2} bar^{-1} and of 97 ± 1% (average values for all the membrane samples used in this study), in agreement with other published results obtained for RO membranes using laboratory scale filtration cells [41–43]. Water permeability during NaCl filtration (determined using Eq. (2)) was observed to be systematically lower than pure water permeability (average decrease of 15%). Doubling the cross-flow velocity did not modify the water permeability or salt rejection (results not reported). Higher tangential flow is expected to reduce the bound-

ary layer thickness due to turbulent flow, thus to lower salt build up at the surface of the membrane, although flow regime conditions (Reynolds number for example) in a lab scale apparatus are not easily determined [43]. Upon rinsing the filtration apparatus and membrane with MilliQ water, initial pure water permeability was recovered. Salt concentration polarisation effects could explain in part the observed reversible water permeability variation. Lowering of hydration swelling of polyamide-based membranes when in contact with solutions of increasing NaCl concentration could also account for the observed water permeability decrease during filtration of concentrated NaCl feed solutions [44,45].

In addition, these transfer properties were found to remain unchanged during two successive filtration experiments when the membrane was immersed in MilliQ water (after being removed from the filtration cell following the first filtration step), as confirmed with control tests. Furthermore, control tests were performed at the start, half way and at the end of the experimental campaign to verify the stability of pristine membrane transfer properties over the time span of the experimental campaign (Fig. 1).

3.2. Chemical analysis of support layers of aged membranes

Previous studies have often implicitly related transfer properties modifications of commercially available composite RO membranes to polyamide chemical transformations, when exposed to chlorine, as we will confirm in the following paragraphs [28,29]. However, analysis of support layers (found in composite membranes) such as polysulfone (PSu), known to react with NaOCl [46,47], should also be performed.

PSu chemical and elemental composition before and after immersion in chlorine baths (4000 ppm h NaOCl concentration and at pH 6.9 and 8.0, most severe ageing conditions applied during our study) was monitored using ATR-FTIR and XPS. To avoid any interferences or overlapping with polyamide and surface layer IR bands and XPS peaks, spectrochemical analysis was performed directly on the PSu layer after peeling off the polyester backing layer of aged membranes. No chlorine was detected on the PSu layer, while chlorine was present on the polyamide layer of the same membrane using XPS (results not shown). Furthermore, known IR band modifications, namely the appearance of a peak at 1034 cm^{-1} assigned to the formation of sulfonic acid due to chain scission of the PSu backbone [47,48], were not observed.

To further confirm the fact that polyamide was the only polymer of our composite membrane to be chemically modified in the chlorine ageing conditions used in our study, the PSu layer (after peeling off the polyester backing layer) was directly put into contact with chlorine. Spectra obtained from XPS, ATR-FTIR and ^{13}C RMN, specifically used for this test, revealed the absence of chemical or elemental modifications of the immersed PSu layer.

4. Results

4.1. Membrane pure water permeability

The effect of membrane exposure to chlorine on the pure water permeability was monitored for doses of 40, 100, 400, 700, 1000, 2500 and 4000 ppm h free chlorine at pH 6.9 and 8.0. Filtration experiments were performed in triplicates for each chlorine dose at both pH values (results not shown).

In brief, two general variations of stabilized pure water permeability were observed.

Below chlorine doses of 400 ppm h, stabilized pure water permeability of aged membranes was on average 50% and 35% higher than values initially obtained for the same membrane prior to ageing, respectively, after contact with chlorine doses of 40 and

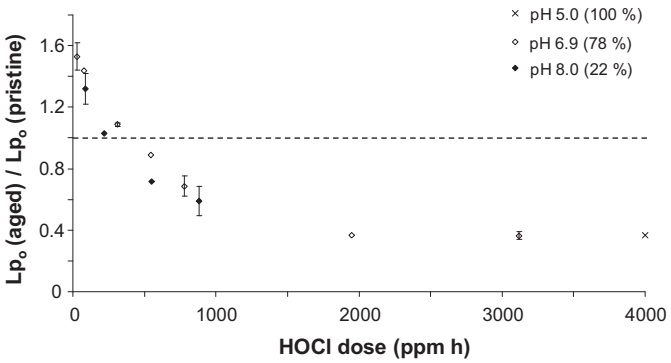

Fig. 2. Relative stabilized pure water permeability as a function of various HOCl doses (converted from chlorine dose values used in this study using molecular percentages for HOCl at pH 5.0, 6.9 and 8.0, as indicated in the graph).

100 ppm h, and without modification of the filtration time necessary to achieve stable pure water permeation conditions. At 400 ppm h and higher, stabilized pure water permeability values of aged membranes decreased by 9% (at 400 ppm h) and up to 64% (at 4000 ppm h), while the filtration time decreased, respectively, to 4 h and 2 h or less. The decrease was more important for both parameters with increasing chlorine dose. Membrane packing was reported to be the dominant impact of chlorine ageing at chlorine doses of 400 ppm h and higher, as observed from the filtration results.

In addition, pure water permeability was found to more severely changed in acidic pH ageing conditions at a given chlorine dose. This is consistent with the reaction mechanism studied on aromatic polyamide model compounds [18,19] and published results on the filtration performance of commercially available membranes [26].

To go further in the analysis of these results, the relative pure water permeability values were expressed vs. the mass concentration of HOCl (Fig. 2). An experimental value obtained at pH 5.0 (HOCl fraction of 100%) was added to the graph for additional comparison. Pure water permeability variations (in both area, <400 ppm h and above 400 ppm h) followed a similar trend, regardless of the pH used for the preparation of the chlorine ageing solution. As presented previously, pure water permeability variations can be described by two trends, separated into two areas depending on the HOCl dose of exposure. The threshold value found in this study is ca. 400 ppm h HOCl (Fig. 2).

Data further seemed to indicate that the relative decrease of pure water permeability leveled off at HOCl doses of 2000 ppm h and up to 4000 ppm h, where maximum packing (stabilized pure water permeability and filtration time) at the applied pressure was reached.

HOCl could be the free chlorine form responsible for the observed membrane packing, by modifying the chemical composition and chain interactions of the polyamide active layer.

Subsequent reverse osmosis of 0.55 M NaCl solutions (at a constant permeation flux of 31 $L\,h^{-1}\,m^{-2}$) was performed for each ageing condition to determine the aged membrane stable salt rejection rates. In brief, salt rejection decreased by less than 1% for ageing conditions below a chlorine dose of 400 ppm h and between 2 and 6% for doses of 400 ppm h and higher (data given for pH 6.9), consistent with variations observed for other commercially available RO membranes exposed to chlorine [15,29] or monochloramine solutions [39].

4.2. Intermolecular hydrogen bond interactions

4.2.1. Peak assignment

Over the range of IR wave numbers scanned, three main distinctive bands could be assigned to aromatic polyamide functional

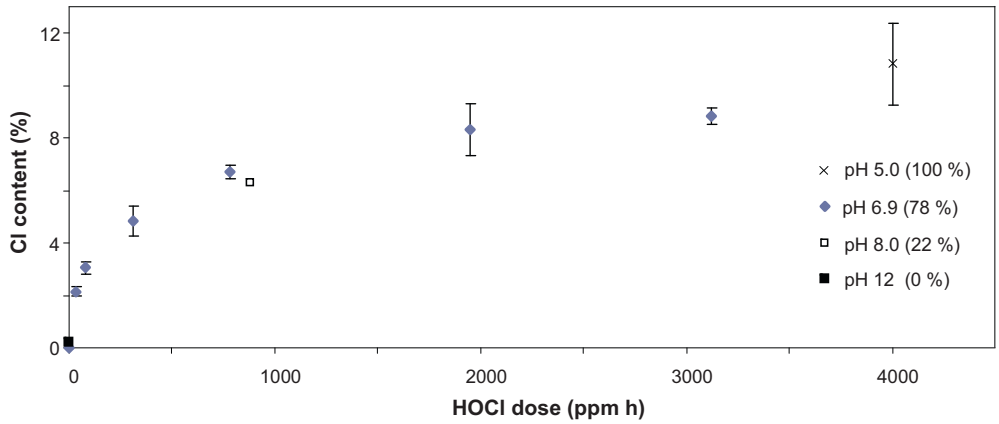

Fig. 3. XPS high resolution scan results of chlorine, Cl (2p) performed on polyamide membranes exposed to varying chlorine doses during 1 h and at pH 5.0, 6.9, 8.0 and 12 (average of 15 scans) – results expressed vs. HOCl dose.

group vibrations: amide I at 1660 cm^{-1}, amide II at 1541 cm^{-1} and a band at 1609 cm^{-1} [49]. This is consistent with findings from a comprehensive work on the identification of polyamide specific IR absorbance bands of numerous commercially available RO composite membranes recently conducted [50].

The amide I mode was reported to combine contributions from the C=O stretching (predominant), the C–N stretching, and the C–C–N deformation vibrations [29,32,51]. In the same articles, the amide II mode at 1541 cm^{-1} was described to have contributions from the *trans* N–H in-plane bending, and the C–N stretching vibrations of the secondary amide group. Finally, the band at 1609 cm^{-1}, assigned to the C=C stretching vibrations for meta-substituted aromatic cycles [49], was furthermore suggested to be linked to the m-phenylenediamine constituent [29,50].

In their studies on the weakening of hydrogen bonding interactions with rise in temperature of fully amorphous or semi-crystalline aliphatic polyamides, Skrovanek et al. indicated that the amide I mode is conformationally sensitive, e.g., that its absorbance frequency is influenced by local interactions such as hydrogen bonding [32,33].

4.2.2. *Effect of ageing conditions*

Consistent with results observed at the macro scale (filtration experiments in this study and reported in the literature), ATR-FTIR spectra of membranes exposed to chlorine baths at a constant dose of 4000 ppm (at the four pH values used in this study), showed that modifications of the three aromatic polyamide bands appeared and were more severe with a decrease of the pH ageing conditions. In brief, the frequencies of the amide I and II modes underwent a shift and the intensities of the absorbance of the amide II mode and of the band at 1609 cm^{-1} decreased (results not shown). No peak modification was noticed for membranes aged at pH 12, where HOCl is non-existent. Atomic percentages obtained with XPS provided additional elements supporting conclusions on the effect of pH, i.e., on the percentage of the free chlorine active specie, and of chlorine concentration on the ageing of aromatic polyamide RO membranes (Fig. 3).

The IR spectra (1000–1800 cm^{-1} region) of membranes exposed to various chlorine doses at pH 6.9 are given in Fig. 4. As an illustration, spectra for which peak evolutions can be visually discerned are presented. Spectra are superimposed to improve visual observation of peak absorbance intensity decrease and/or shift in frequency.

As the chlorine dose in the immersion bath increased in a stepwise fashion, the amide I at 1660 cm^{-1} (associated mainly to C=O stretching) shifted progressively to higher frequency, the amide II at 1541 cm^{-1} (associated mainly to *trans* N–H deformation) shifted to lower frequency and the absorbance intensity decreased. The absorbance intensity of the band at 1609 cm^{-1} progressively decreased with increasing chlorine dose. These observations are consistent with results found for different commercially available RO composite membranes in comprehensive studies published by Kwon et al. [29,30]. The authors also suggested that amide I and II peak variations were associated with breakage of intermolecular C=O···H–N hydrogen bond interactions, due to the electrophilic substitution of N–H by N–Cl, first step of the identified chlorination mechanism of aromatic polyamide [18,19,22].

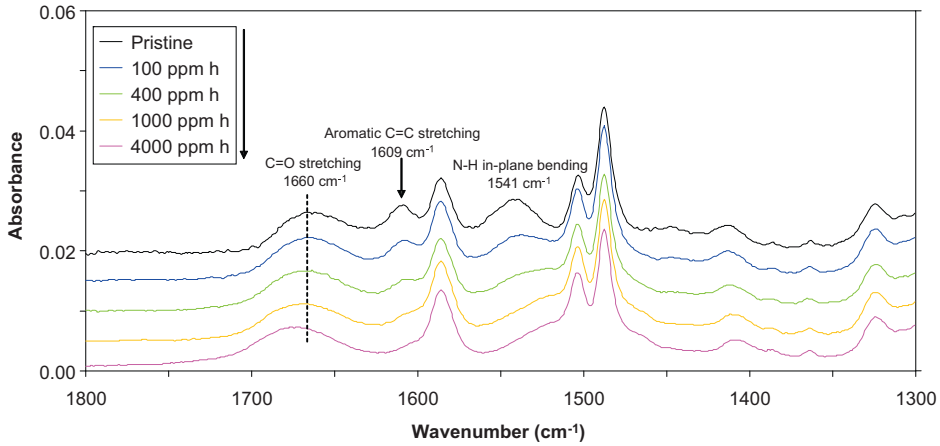

Fig. 4. ATR-FTIR spectra of pristine membranes and membranes exposed to free chlorine at 100, 400, 1000 and 4000 ppm h at pH 6.9.

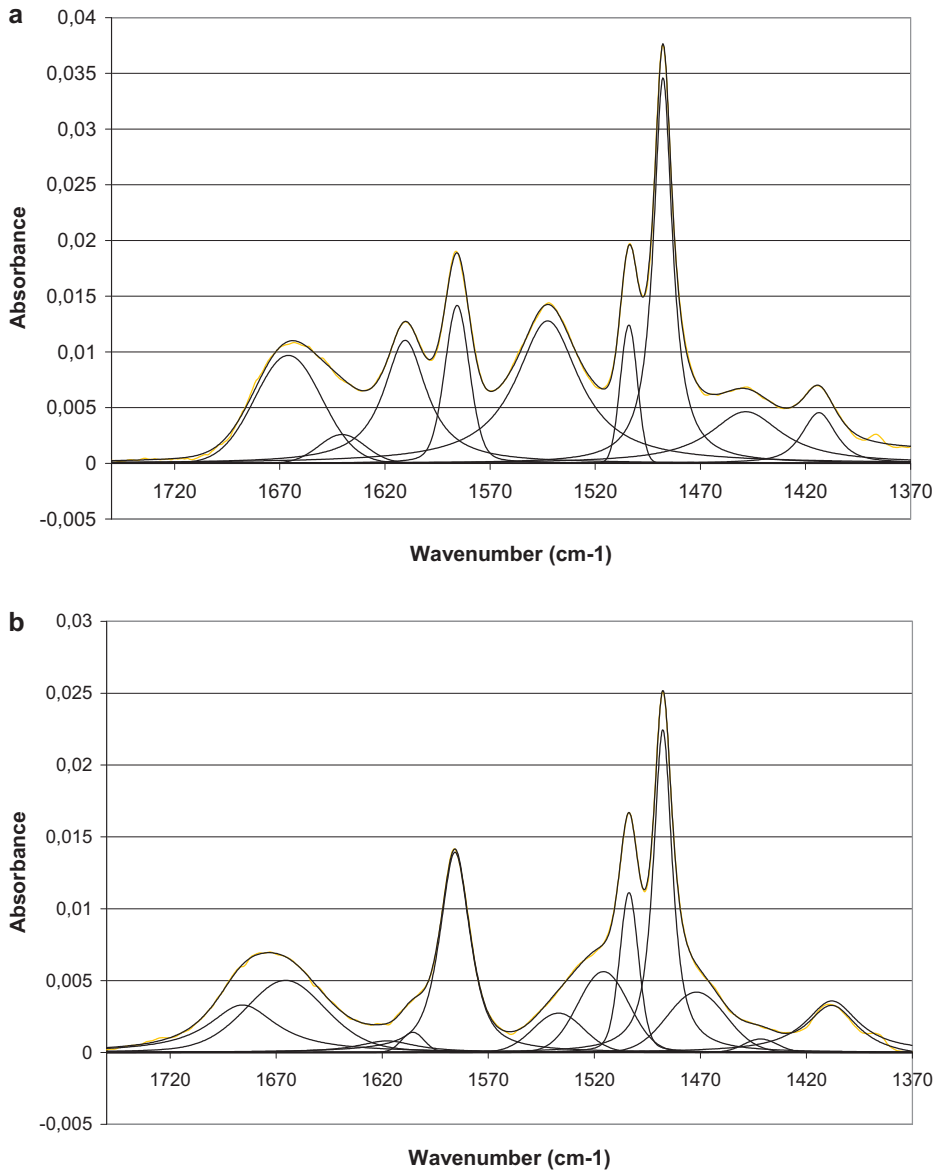

Fig. 5. ATR-FTIR original, fitted and deconvoluted spectra recorded in the range 1370–1750 cm^{-1} of a pristine membrane (a) and exposed to a chlorine dose of 4000 ppm h, at pH 6.9 (b).

Additionally, the amide I band width also increased with increasing chlorine concentration, without noticeable variation of the absorbance intensity, conferring to the peak a growing asymmetric shape. The shift in frequency could be attributed to the variation in intensity of hydrogen bonded C=O, at 1660 cm^{-1}, and of non-associated C=O bonds, at 1680 cm^{-1} [49]. Inspired by curve fitting procedures applied in studies of Skrovanek et al. [32,33], we performed a deconvolution of the amide I band. This functional group is not a reactive constituent of the 2 step electrophilic substitution chlorination mechanism of aromatic polyamide [22]. In addition, as mentioned earlier, the amide I bond was reported to be sensitive to conformational order, which we agree to believe was changed with chlorine exposure in our ageing conditions, and could thus provide concluding insights on the hypothesized weakening of aromatic polyamide hydrogen bond interactions [29,30].

4.2.3. Curve fitting

Curve fitting was performed in the range 1370–1750 cm^{-1} of IR recorded spectra described previously. The range chosen for the deconvolution included the aromatic polyamide amide II and band at 1609 cm^{-1} as well as present polysulfone bands. This was performed to obtain a linear base line where no underlying bands were found in the IR frequency range of interest. Based on the settings of Skrovanek et al. [33] done with aliphatic semi-crystalline polyamide polymers (Nylon 11), the amide I mode was assumed to be composed of three bands assigned to the hydrogen bonded C=O groups in the ordered domains (1640 cm^{-1}), hydrogen bonded C=O groups in the disordered domains (1660 cm^{-1}), and non-associated C=O groups (1680 cm^{-1}). Both Gaussian and Lorentz distributions were considered for the area studied. Results of the calculations are given below (Fig. 5):

- width at mid height of the peaks remained constant with ageing conditions ($W_{1/2}$ (1640 cm^{-1}) = 30 ± 3 cm^{-1}; $W_{1/2}$ (1660 cm^{-1}) = 38 ± 2 cm^{-1}; $W_{1/2}$ (1680 cm^{-1}) = 20 ± 2 cm^{-1})
- the shape of the bands at 1680 and 1660 cm^{-1} were modeled by Gaussian distribution (~80% contribution) and Lorentz distribution (~20%), these parameters not being fixed for the calculations.

By comparing the area of the C=O hydrogen bonded fractions in the ordered and disordered domains, it appeared that the band at 1660 cm^{-1} strongly contributed to the overall amide I band of pristine membranes.

In addition, for a given sample, the method used for peak fitting assumed that the extinction coefficient for the amide I vibration band was similar for the different components obtained from the deconvolution of the amide I mode.

Peak area modifications could thus be attributed to absorbance intensity variations. The progressive shift in frequency of the amide I band (Fig. 4) with increasing free chlorine concentration seems to be associated to the relative increase of the fraction of non associated carbonyl groups at 1680 cm^{-1} and decrease of the fraction of hydrogen bonded carbonyl groups in the disordered domains at 1660 cm^{-1}, as suggested by the trends presented in Fig. 6. Due to irregular variations in the total peak area of aged samples, fractions of each peak obtained during the deconvolution of pristine and membranes exposed to free chlorine are presented to normalize their evolution with the chlorine dose (Fig. 6b). The trend obtained in Fig. 6b seems to support the previous statement.

Deconvolution of the amide I band reveals that exposure of aromatic polyamide-based RO membranes to chlorine could thus result in the weakening of intermolecular hydrogen bond interactions.

Negligible variations of the area of the hydrogen bonded carbonyl groups in the ordered domains at 1640 cm^{-1} were observed. Diffusion of the chlorine solutions through the polyamide layer and subsequent reaction with the latter's functional groups was expected to occur in the disordered domains, in agreement with published data [13]. It is difficult to provide unequivocal assumptions based on these results, given the relative low contribution of the 1640 cm^{-1} peak to the amide I band (from our study).

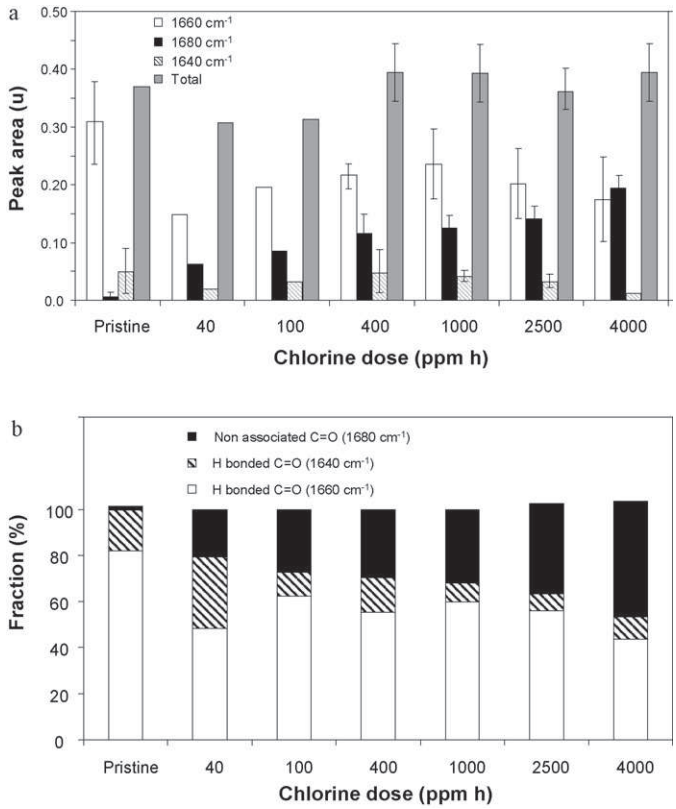

Fig. 6. Results of the deconvolution performed on the amide I band. (a) Areas of the disordered (white) and ordered (dashed) hydrogen bonded and non associated (black) carbonyl groups and (b) fraction of each deconvoluted peak of pristine and membranes exposed to various free chlorine doses (ageing performed at pH 6.9).

5. Change in polyamide conformational order with exposure to chlorine

Deconvolution of ATR-FTIR obtained amide I band showed that the response of initially pristine aromatic-polyamide based RO membranes to increasing chlorine exposure (dose, pH) lead to systematic weakening of intermolecular hydrogen bond interactions (Fig. 6). These results correlate well with pure water permeability values.

Membrane packing, suggested by the decrease of the relative pure water permeability, occurred and progressed for fractions of non associated carbonyl groups higher than 30% (corresponding to a dose of 400 ppm h at pH 6.9), as shown in Fig. 7. Growing membrane response to mechanical stress, generated during pressurized filtration of pure water, was observed above this threshold. However, we could not dissociate in our experiments the impact of pure water absorption from that of pressure on the structure of chlorine exposed polyamide. Even though RO polyamide membranes were reported to be negligibly swelled in water due to the rigidity of the polymer [45], uptake of water, associated with compressive bi-axial stress, was shown to result in permanent polymer deformation [52,53]. Hence, water absorption could contribute to the modification of chain conformation, as also reported for model nylon films [35,54].

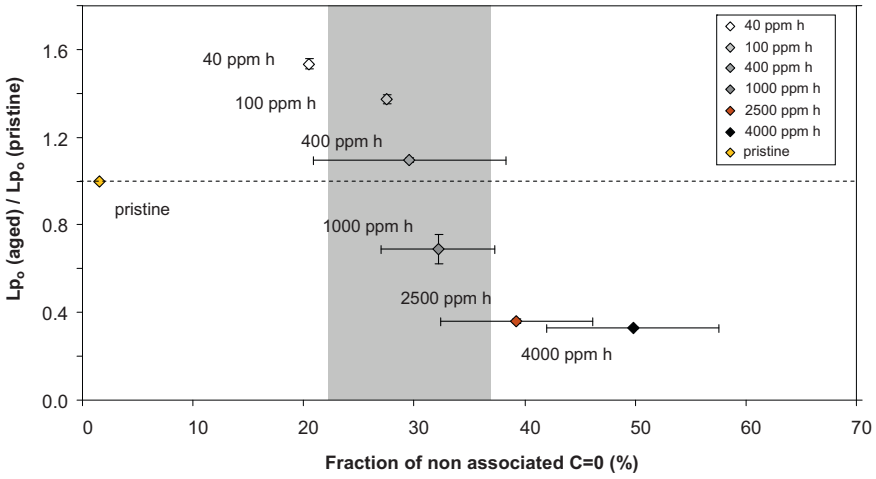

Fig. 7. Relative pure water permeability plotted vs. the fraction of non associated carbonyl groups of pristine and membranes exposed to chlorine doses of 40, 100, 400, 1000, 2500 and 4000 ppm h at pH 6.9.

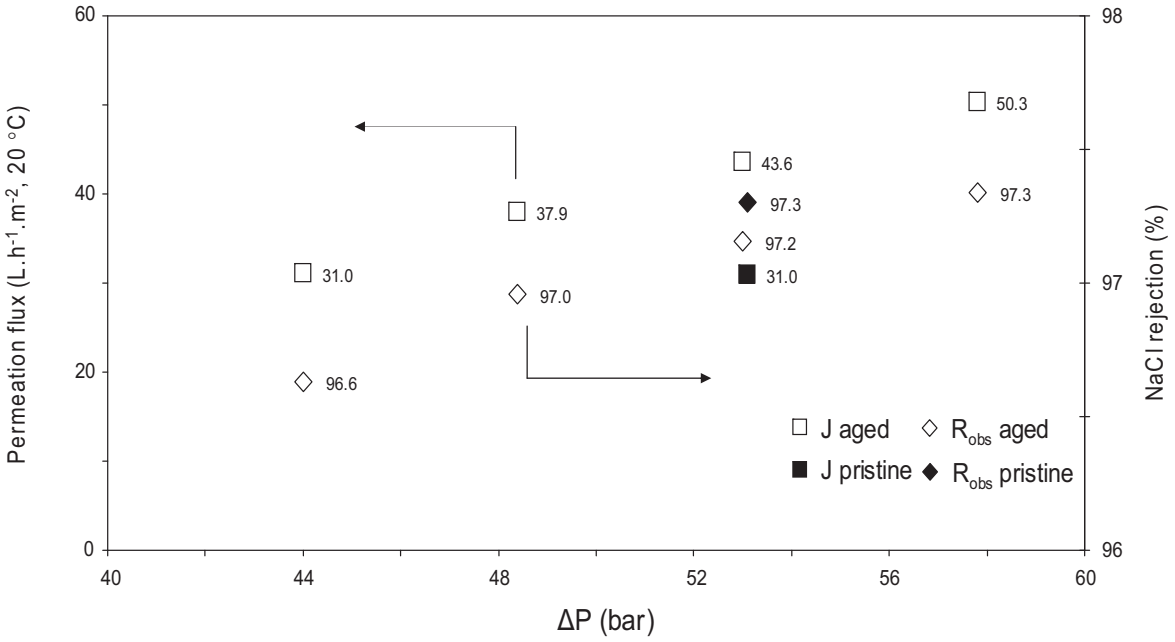

Fig. 8. NaCl rejection rate (diamond) and water permeation flux (square) vs. applied pressure of an initially pristine membrane (black), then exposed to chlorine at 100 ppm h, pH 6.9 (white).

From a mechanistic point of view, the weakening of intermolecular hydrogen bond interactions seemed to cause an increase of the packing propensity of the membranes, by increasing the mobility of the structure as hypothesized elsewhere [29,30]. Techniques other than ATR-FTIR would be needed to monitor the conformational changes of chlorine exposed polyamides. Thermal and X-ray diffraction analysis were used to obtain such information for electrospun nylon 6 membranes containing prechlorinated N-halamines. Results of this study revealed that the incorporation of N-halamines caused a change in the crystalline phase from an α stable form to a γ meta stable form resulting in a decrease of the melt temperature, presumed to be associated with the decrease of nylon intermolecular hydrogen bonds [55].

For lower chlorine doses, increase of both the fraction of non associated carbonyl groups and of relative pure water permeability was observed (Fig. 7), seemingly in contradiction with the packing propensity of the membranes. Other impacts resulting from chlorine incorporation, in addition to structural changes, could include modifications in the interactions of chlorinated polyamide functional groups with environing elements, thus impacting on the solubility of species at the polyamide surface layer. Sessile drop contact angle measurements published elsewhere showed an increase of the hydrophilicity [27,28]. *Ab initio* molecular calculations, which could provide relevant insights, were used to analyze the (weak) hydrogen bond acceptor behavior of C–Cl, e.g., participating in C–Cl···H–N(–O) [56,57]. At these lower doses, different physical and chemical property changes could come into play and influence pure water permeability values. However, increase of pure water permeability and of salt transfer across membranes exposed to 40–100 ppm h doses (at pH 6.9) could be explained by a loss of polyamide chain rigidity (to a lower degree than for higher chlorine doses), which allows the distortion of polyamide chains, to accommodate for a higher diffusion of hydrated salts (permeate salt concentration was on average less than 4% of a 0.55 M NaCl bulk solution), but does not affect polyamide stability to applied pressure.

This is consistent with recent work that found that salt penetration (for concentrations ranging from 10^{-4} to 1 M NaCl) in model nylon films could be achieved in free volumes generated by swelling with water absorption, the authors assuming that water could participate in the hydration of both nylonchains and of salt ions [35].

In addition, there seems to be no contradiction with results on the systematic decrease of the water permeability (A) of rigid polyamide-based NF membranes with increasing NaCl concentration found by Freger and co-workers [44]. In this case, competitive hydration between salt ions and polyamide functional groups in a rigid structure was involved. This latter behavior was observed in our study during control filtration experiments where membranes were immersed in similarly prepared baths but without chlorine.

The main ageing mechanism induced by chlorine exposure of polyamide-based RO membranes was believed to be associated with polymer chain mobility (amongst other physical and chemical property changes that could contribute at low chlorine doses). With strengthening of chlorine exposure conditions (chlorine dose and solution pH), ability of polyamide chains to undergo conformational evolutions under mechanical stress induced by the application of high pressure or by diffusion of hydrated salt ions [15,29] was thought to increase due to progressive weakening of polyamide intermolecular hydrogen bond interactions.

Under the lowest chlorine exposure conditions used during this study, i.e., below a HOCl dose of 100 ppm h, it was observed that the applied pressure required to achieve a constant permeation flux decreased by ca. 17% due to an increase of water permeability (A), compared with operating conditions used for the same membrane initially pristine (Fig. 8). Alternatively, permeation flux can be increased by ca. 40% (with the same applied pressure) while achieving comparable sodium chloride rejection capabilities (Fig. 8).

6. Conclusions

Aromatic polyamide membrane structure property modifications with exposure to varying chlorine ageing conditions were assessed in this study. In agreement with previous studies performed on commercially available RO membranes, we found that the weakening of polyamide intermolecular hydrogen bonds is a main consequence of chlorine ageing of aromatic polyamide RO membranes, particularly affecting membrane transfer properties. Macro scale analysis, i.e., membrane hydraulic resistance measure-

ments obtained from DI water filtration experiments and ATR-FTIR chemical composition analysis were observed to be sensitive to different chlorine ageing conditions used in this study (chlorine dose and solution pH) and provided complementary insights on the modification of polyamide structure properties. Main findings of this study are summarized as follows.

- Aromatic polyamide thin film was shown to be the only polymer layer of the composite RO membrane chemically modified in the accelerated chlorine ageing conditions used
- Hypochlorous acid is the free chlorine specie active in the chlorination of aromatic polyamide in the pH range used in this study (>pH 5)
- Deconvolution (under conditions used in this study) of the IR vibrational amide I band, comprising a main contribution of the carbonyl bond non affected by the chlorination mechanism, unveiled an increase in the fraction of non associated C=O groups ($1680\,cm^{-1}$) and a decrease of H bonded C=O groups in the disordered domains of the semi-crystalline polyamide ($1660\,cm^{-1}$)
- Weakening of polyamide intermolecular H bonds is believed to affect conformational order in the crosslinked aromatic polyamide as observed particularly with the packing propensity dominant at high hypochlorous acid concentrations and with the increase of salt passage
- A threshold value for the fraction of non-associated C=O groups, ca. 30%, above which polyamide based RO membrane packing propensity is initiated
- An HOCl dose of ca. 400 ppm h corresponds to chlorine exposure conditions (free chlorine dose, solution pH) above which permanent RO membrane performance loss (water permeability and rejection) is expected.

Furthermore, as observed during accelerated ageing campaigns used to simulate eventual chlorine exposure on-site, pure water filtration tests and ATR-FTIR analysis were found to be sensitive techniques and relevant for the characterization of chlorine-aged aromatic polyamide RO membranes, readily applied in autopsy-expertise studies.

Acknowledgments

The authors wish to thank Corinne Routaboul from the Infrared and Raman department of the Université Paul Sabatier of Toulouse for ATR-FTIR analysis and helpful discussions concerning the results of the spectra deconvolutions. We also wish to thank Valérie Flaud from ICG Montpellier for performing XPS analysis.

Veolia Environnement is gratefully acknowledged for funding this work.

References

[1] J.E. Cadotte, R.S. King, R.J. Majerle, R.J. Petersen, Interfacial synthesis in the preparation of reverse osmosis membranes, Journal of Macromolecular Science: Chemistry A15 (1981) 727–755.
[2] R.E. Kesting, Synthetic Polymeric Membranes, Mcgraw-Hill Book Company, 1971.
[3] M. Mulder, Basic Principles of Membrane Technology, second ed., Kluwer Academic Publishers, Dordrecht, 1996.
[4] E.M.V. Hoek, M. Elimelech, Cake-enhanced concentration polarization: a new fouling mechanism for salt-rejecting membranes, Environmental Science and Technology 37 (2003) 5581–5588.
[5] C. Bellona, J.E. Drewes, P. Xu, G. Amy, Factors affecting the rejection of organic solutes during NF/RO treatment – a literature review, Water Research 38 (2004) 2795–2809.
[6] M. Herzberg, M. Elimelech, Biofouling of reverse osmosis membranes: role of biofilm-enhanced osmotic pressure, Journal of Membrane Science 295 (2007) 11–20.
[7] N. Prihasto, Q.-F. Liu, S.-H. Kim, Pre-treatment strategies for seawater desalination by reverse osmosis system, Desalination 249 (2009) 308–316.
[8] C. Astudillo, J. Parra, S. González, B. Cancino, A new parameter for membrane cleaning evaluation, Separation and Purification Technology 73 (2010) 286–293.
[9] A.J. Gijsbersten-Abrahamse, E.R. Cornelissen, J.A.M.H. Hofman, Fiber failure frequency and causes of hollow fiber integrity loss, Desalination 194 (2006) 251–258.
[10] E. Zondervan, A. Zwijnenburg, B. Roffel, Statistical analysis of data from accelerated ageing tests of PES UF membranes, Journal of Membrane Science 300 (2007) 111–116.
[11] T. Knoell, E. Martin, K. Ishida, D. Phipps, The effect of chlorine exposure on the performance and properties of polyamide reverse osmosis membranes, in: Awwa Membrane Technical Conference Proceedings, 2005.
[12] J.E. Cadotte, R.J. Petersen, R.E. Larson, E.E. Erickson, A new thin-film composite seawater reverse osmosis membrane, Desalination 32 (1980) 25–31.
[13] S. Avlonitis, W.T. Hanbury, T. Hodgkiess, Chlorine degradation of aromatic polyamides, Desalination 85 (1992) 321–334.
[14] S. Wu, J. Xing, G. Zheng, H. Lian, L. Shen, Chlorination and oxidation of aromatic polyamides. II. Chlorination of some aromatic polyamides, Journal of Applied Polymer Science 61 (1996) 1305–1314.
[15] C.J. Gabelich, J.C. Frankin, F.W. Gerringer, K.P. Ishida, I.H. Suffet, Enhanced oxidation of polyamide membranes using monochloramine and ferrous ion, Journal of Membrane Science 258 (2005) 64–70.
[16] Dow Filmtec Technical Manual, 2005, July, p. 60.
[17] http://www.membranes.com/.
[18] J.E. Glater, S.-K. Hong, M. Elimelech, The search for a chlorine-resistant reverse osmosis membrane, Desalination 95 (1994) 325–345.
[19] N.P. Soice, A.C. Maladono, D.Y. Takigawa, A.D. Norman, W.B. Krantz, A.R. Greenberg, Oxidative degradation of polyamide reverse osmosis membranes: studies of molecular model compounds and selected membranes, Journal of Applied Polymer Science 90 (2003) 1173–1184.
[20] L. Abia, X.L. Armesto, M. Canle, M.V. García, J.A. Santaballa, Oxidation of aliphatic amines by aqueous chlorine, Tetrahedron 54 (1998) 521–530.
[21] J.S. Jensen, Y.-F. Lam, G.R. Helz, Role amide nitrogen in water chlorination: proton NMR evidence, Environmental Science and Technology 33 (1999) 3568–3573.
[22] A. Akdag, H.B. Kocer, S.D. Worley, R.M. Broughton, T.R. Webb, T.H. Bray, Why does Kevlar decompose, while Nomex does not, when treated with aqueous chlorine solutions? Journal of Physical Chemistry B 111 (2007) 5581–5586.
[23] N. Dam, P.R. Ogilby, On the mechanism of polyamide degradation in chlorinated water, Helvetica Chimica Acta 84 (2001) 2540–2549.
[24] P. Tarakeshwar, J.Y. Lee, K.S. Kim, Role of Lewis acid ($AlCl_3$)–aromatic ring interactions in Friedel-Craft's reaction: an ab initio study, The Journal of Physical Chemistry A 102 (1998) 2253–2255.
[25] J.C. Lozier, Evaluating chloramines for control of RO membrane biofouling with ground and surface water supplies, in: Awwa Membrane Technology Conference Proceedings, 2005.
[26] J-Y. Koo, J.H. Lee, Y.D. Jung, S.P. Hong, S.R. Yoon, Chlorine resistant membrane and the mechanism of membrane degradation by chlorine, in: Awwa Membrane Technology Conference Proceedings, 2009.
[27] Y.-N. Kwon, J.O. Leckie, Hypochlorite degradation of crosslinked polyamide membranes. I. Changes in chemical/morphological properties, Journal of Membrane Science 283 (2006) 21–26.
[28] A. Simon, L.D. Nghiem, P. Le-Clech, S.J. Khan, J.E. Drewes, Effects of membrane degradation on the removal of pharmaceutically active compounds (PhACs) by NF/RO filtration processes, Journal of Membrane Science 340 (2009) 16–25.
[29] Y.-N. Kwon, J.O. Leckie, Hypochlorite degradation of crosslinked polyamide membranes. II. Changes in hydrogen bonding behavior and membrane performance, Journal of Membrane Science 282 (2006) 456–464.
[30] Y.-N. Kwon, C.Y. Tang, J.O. Leckie, Change of chemical composition and hydrogen bonding behavior due to chlorination of crosslinked polyamide membranes, Journal of Applied Polymer Science 108 (2008) 2061–2066.
[31] G. De Luca, A. Gugliuzza, E. Drioli, Competitive hydrogen-bonding interactions in modified polymer membranes: a density functional theory investigation, Journal of Physical Chemistry B 113 (2009) 5473–5477.
[32] D.J. Skrovanek, S.E. Howe, P.C. Painter, M.M. Coleman, Hydrogen bonding in polymers: infrared temperature studies of an amorphous polyamide, Macromolecules 18 (1985) 1676–1683.
[33] D.J. Skrovanek, P.C. Painter, M.M. Coleman, Hydrogen bonding in polymers. 2. Infrared temperature studies of an Nylon 11, Macromolecules 19 (1986) 699–705.
[34] N. Sanjeeva Murthy, Hydrogen bonding, mobility, and structural transitions in aliphatic polyamides, Journal of Polymer Science Part B: Polymer Physics 44 (2006) 1763–1782.
[35] C.J. Orendorff, D.L. Huber, B.C. Bunker, Effects of water and temperature on conformational order in model nylon thin films, Journal of Physical Chemistry C 113 (2009) 13723–13731.
[36] S. Rapenne, Dessalement D'eaux de mer par Osmose Inverse: Impact des Procédés Conventionnels sur les Caractéristiques Physicochimiques et Microbiologiques de la Ressource et Étude du Colmatage, Université de Poitiers, France, 2007.
[37] P.N. Tanki, R.P. Singh, Photo-oxidative degradation of nylon 66 under accelerated weathering, Polymer 39 (1998) 6363–6367.
[38] D.S. Rosa, J.M.G. Angelini, J.A.M. Agnelli, L.H.I. Mei, The use of optical microscopy to follow the degradation of isotactic polypropylene (PP) subjected to natural and accelerated ageing, Polymer Testing 24 (2005) 1022–1026.

[39] M.K. da Silva, I.C. Tessaro, K. Wada, Investigation of oxidative degradation of polyamide reverse osmosis membranes by monochloramine solutions, Journal of Membrane Science 282 (2006) 375–382.
[40] J. Glater, M.R. Zachariah, S.B. McCray, J.W. McCuthan, Reverse osmosis membrane sensitivity to ozone and halogen disinfectants, Desalination 48 (1983) 1–16.
[41] C.Y. Tang, Y.-N. Kwon, J.O. Leckie, Effect of membrane chemistry and coating layer on physicochemical properties of thin film composite polyamide RO and NF membranes. II. Membrane physicochemical properties and their dependence on polyamide and coating layers, Desalination 242 (2009) 168–182.
[42] S.T. Mitrouli, A.J. Karabelas, N.P. Isaias, Polyamide active layers of low pressure RO membranes: data on spatial performance non-uniformity and degradation by hypochlorite solutions, Desalination 260 (2010) 91–100.
[43] E.M. Van Wagner, A.C. Sagle, M.M. Sharma, B.D. Freeman, Effect of crossflow testing conditions, including feed pH and continuous feed filtration, on commercial reverse osmosis membrane performance, Journal of Membrane Science 345 (2009) 97–109.
[44] V. Freger, T.C. Arnot, J.A. Howell, Separation of concentrated organic/inorganic salt mixtures by nanofiltration, Journal of Membrane Science 178 (2000) 185–193.
[45] V. Freger, Swelling and morphology of the skin layer of polyamide composite membranes: an atomic force microscopy study, Environmental Science and Technology 38 (2004) 3168–3175.
[46] S. Rouaix, C. Causserand, P. Aimar, Experimental study of the effects of hypochlorite on polysulfone membrane properties, Journal of Membrane Science 277 (2006) 137–147.
[47] E. Gaudichet-Maurin, F. Thominette, Ageing of polysulfone ultrafiltration membranes in contact with bleach solutions, Journal of Membrane Science 282 (2006) 198–204.
[48] K. Yadav, K. Morison, M.P. Staiger, Effects of hypochlorite treatment on the surface morphology and mechanical properties of polyethersulfone ultrafiltration membranes, Polymer Degradation and Stability 94 (2009) 1955–1961.
[49] G. Socrates, Infrared and Raman Characteristic Group Frequencies, third ed., Wiley, 2001.
[50] C.Y. Tang, Y.-N. Kwon, J.O. Leckie, Effect of membrane chemistry and coating layer on physicochemical properties of thin film composite polyamide RO and NF membranes. I. FTIR and XPS characterization of polyamide and coating layer chemistry, Desalination 242 (2009) 149–167.
[51] R.D. McLachlan, R.A. Nyquist, An infrared study of some α-substituted secondary amides in solution, Spectrochimica Acta 20 (1964) 1397–1406.
[52] I.J. Roh, J.-J. Kim, S.Y. Park, Mechanical properties and reverse osmosis performance of interfacially polymerized polyamide thin films, Journal of Membrane Science 197 (2002) 199–210.
[53] X. Zhang, D.G. Cahill, O. Coronell, B.J. Mariñas, Absorption of water in the active layer of reverse osmosis membranes, Journal of Membrane Science 331 (2009) 143–151.
[54] V. Miri, O. Persyn, J.-M. Lefebvre, R. Seguela, Effect of water absorption on the plastic deformation behaviour of nylon 6, European Polymer Journal 45 (2009) 757–762.
[55] K. Tan, S. Kay Obendorf, Fabrication and evaluation of electrospun nanofibrous antimicrobial nylon 6 membranes, Journal of Membrane Science 305 (2007) 287–298.
[56] G. Aullón, D. Bellamy, L. Brammer, E.A. Bruton, A. Guy Orpen, Metal-bound chlorine effect often accepts hydrogen bonds, Chemical Communications 6 (1998) 653–654.
[57] L. Brammer, E.A. Bruton, P. Sherwood, Understanding the behaviour of halogens as hydrogen bond acceptors, Crystal Growth and Design 1 (2001) 277–290.